scientific reports

Check for updates

OPEN

Proliferative and viability effects of two cyanophages on freshwater bloom-forming species *Microcystis aeruginosa* and *Raphidiopsis raciborskii* vary between strains

Nada Tokodi[1,2], Antonia Łobodzińska[1], Barbara Klimczak[1,3], Adam Antosiak[1,3], Sara Młynarska[1], Sigitas Šulčius[4], Sarit Avrani[5], Takashi Yoshida[6,7] & Dariusz Dziga[1]✉

Viruses that infect cyanobacteria are an integral part of aquatic food webs, influencing nutrient cycling and ecosystem health. However, the significance of virus host range, replication efficiency, and host compatibility on cyanobacterial dynamics, growth, and toxicity remains poorly understood. In this study, we examined the effects of cyanophage additions on the dynamics and activity of optimal, sub-optimal, and non-permissive cyanobacterial hosts in cultures of *Microcystis aeruginosa* and *Raphidiopsis raciborskii*. Our findings reveal that cross-infectivity can substantially reduce the proliferative success of the cyanophage under conditions of high-density of sub-optimal hosts which suggests phage dispersal limitation as a result of shared infections, in turn impairing their top-down control over the host community. Furthermore, we found that cyanophage addition triggers host strain-specific responses in photosynthetic performance, population size and toxin production, even among non-permissive hosts. These non-lytic effects suggest indirect impacts on co-existing cyanobacteria, increasing the overall complexity and variance in many ecologically relevant cyanobacterial traits. The high variability in responses observed with a limited subset of cyanophage-cyanobacteria combinations not only highlights the intricate role of viral infections in microbial ecosystems but also underscores the significant challenges in predicting the composition, toxicity, and dynamics of cyanobacterial blooms.

Keywords Harmful cyanobacterial blooms, Freshwater cyanophages, Virus-host interactions, Optimal and suboptimal hosts, *Microcystis aeruginosa*, *Raphidiopsis Raciborskii*

Cyanophages are ubiquitous and abundant members of aquatic microbial food webs, playing a key role in microbial population and community dynamics, and hence mediating and driving nutrient cycling in ecosystems[1]. Cyanophages can affect their hosts in various ways. They affect their population size due to the host lysis[2], promote host population variability through lateral gene transfer[3] and selection for resistant strains[4], and can alter their host metabolism[5–7]. Moreover, cyanophage derived lysis can affect non-host strains in their proximity. For example, phage lysis of the diazotrophic *Nodularia*[8,9], as well as marine cyanobacteria[10], caused the release of fixed nitrogen to the environment, which improved the growth of various non-diazotrophic cyanobacteria and algae strains.

It has been shown that the occurrence of individual viral genotypes/lineages range from sporadic appearance to persistent presence on both spatial and temporal scales[11,12], suggesting varying effect of different viral lineages

[1]Laboratory of Metabolomics, Faculty of Biochemistry, Biophysics and Biotechnology, Jagiellonian University, Gronostajowa 7, Krakow 30387, Poland. [2]Department of Biology and Ecology, Faculty of Sciences, University of Novi Sad, Trg Dositeja Obradovića 3, Novi Sad 21000, Serbia. [3]Doctoral School of Exact and Natural Sciences, Jagiellonian University, Krakow 30-348, Poland. [4]Laboratory of Algology and Microbial Ecology, Nature Research Centre, Akademijos str. 2, Vilnius 08412, Lithuania. [5]Department of Evolutionary and Environmental Biology, Institute of Evolution, University of Haifa, Haifa, Israel. [6]Laboratory of Marine Microbiology, Graduate School of Agriculture, Kyoto University, Kyoto, Japan. [7]School of Environmental Science, University of Shiga Prefecture, Hikone, Japan. ✉email: dariusz.dziga@uj.edu.pl

on the co-occurring community. The underlying mechanisms driving the abundance and dynamics of individual viral genotype/lineage, although remains insufficiently understood, are known to involve a variety of processes and virus traits. These mechanisms include virus host range, efficiency of virus proliferation on different host strains/species (measured as adsorption rate, latent period, and burst size), host and phage availability (including density, micro-diversity and growth stage), host permissiveness[13], as well as virus replication strategy (virulent vs. temperate)[14].

Virus host range, which can be defined as the span of species and strains that support its replication, is a dynamic feature prone to high variability[15,16] owing to spontaneous mutations, fitness effects and strength of selection forces[17]. Most cultured cyanophages have relatively narrow host range, infecting only a host of isolation and/or few other strains within a single species, and with the replication success varying greatly, even across highly similar (>99% sequence similarity) phages[16,18–20]. However, viruses capable of infecting host belonging to different cyanobacterial species or genera have also been isolated from both marine and freshwater environments[21–24].

Cyanophages infecting bloom-forming cyanobacteria experience dramatic changes in their host growth rate, physiological state, and abundance, which can consequently affect various aspects of phage-host interactions. Indeed, it has been shown that both taxonomic composition, activity and cyanophage lifestyle (switch from lytic replication to lysogeny) may change with the bloom phase and host density[25,26]. Moreover, natural blooms consisting of multiple phylo- and genotypes may create a network of virus-host interactions varying in strength and effects over both spatial scale and seasonal changes[26–28]. During the peak of the bloom, for example, the host availability becomes extremely high, which may lead to high infection rates by lytic phages and consequently reduction of host population size[29]. High variability within the cyanobacteria populations and community may not only prevent the collapse of the bloom but also allow the coexistence between viruses and their potential hosts[30]. On the other hand, low density of the bloom-forming species reduces the contact rate between cyanophages and their cyanobacterial hosts, which then diminishes the overall effect of cyanophage infection on the host population and community dynamics.

Under low cyanobacterial abundance a very narrow host range may become a disadvantage[15,31]. On the other hand, broader host range viruses are often associated with lower replication efficiency[32,33]. It is, therefore, reasonable to assume that the abundance of a specific viral genotype in space and time would be determined by virus-host compatibility (see the description of Fig. 1), and that the number of the contacts between the most compatible (optimal) host and a virus would increase with lower population/community diversity and higher density of optimal host cells[34,35]. Therefore, under conditions of the high density of the optimal host, infection efficiency and, hence, the production and abundance of viruses, would be higher compared to the conditions of the high density of a sub-optimal host due to lower virus-host compatibility (Fig. 1). Since virus-host compatibility is a continuous trait[16,30], the level of phage production and abundance will vary. Although at low densities infecting either type of the host would ensure virus survival and transmission, if both optimal and sub-optimal hosts are present at high densities, then the infection efficiency of a virus at population level can be impaired, leading to lower overall yield of newly produced virions in a sub-optimal host, and thus to lower virus prevalence and persistence in the environment (Fig. 1). For example, Wang et al.[36] reported significant reduction and inhibition of virus production when phage was infecting strains other than the original host of its isolation. The growth of other host strains was inhibited after exposure to viruses, likely preventing phage replication that may lead to abortive infection and, therefore, the lack of plaque formations found in this study[36]. This, thus, also suggests that the effect of viral infection of a sub-optimal host may extend beyond regular cell lysis.

The interactions and ecological dynamics between viruses and their cyanobacterial hosts are governed by multiple eco-evolutionary processes[37–39]. Even within the relatively short time frame of a seasonal cyanobacterial succession, these processes can lead to a variety of outcomes, ranging from positive density-dependent interactions and lysogenic conversions during the bloom initiation stages to the near-complete eradication of host populations during bloom decline[2,40]. For example, cyanophages have been implicated as possible causative factor of sudden cyanobacterial bloom collapses in various freshwater ecosystems across the globe[41–45]. Conditions when multiple strains of the same and different species co-occur at high numbers, and which are potentially prone to infection by the same phage can emerge during summer cyanobacterial blooms[26,46]. For example, *Microcystis aeruginosa* (Kützing) Kützing, 1846 and *Raphidiopsis raciborskii* (Wołoszyńska) Aguilera & al. 2018 (two of the most abundant bloom-forming species on earth) are often found together at high densities during summer blooms in freshwater lakes[47]. They are cosmopolitan, and many of their strains form harmful blooms due to their ability to produce various toxins. They are known to bloom in parallel or in alternating manner in different environments[48]. Various cyanophages are known to infect these bloom-forming strains. The vast majority of these phages are host specific[49], however, the way they affect these blooms is still not well understood. Here we aim to (i) assess the dynamics of virus-host pairs in the context of availability of optimal versus sub-optimal host belonging to *Microcystis aeruginosa* and *Raphidiopsis raciborskii* species (Fig. 1); (ii) verify how these phages (Cr-LKS4 and Ma-LMM01) affect the functionality (growth and photosynthetic activity) of the strains used for their isolation (KLL07 and NIES-298, respectively) and other strains of these species; (iii) determine if and to which extent the toxicity of investigated strains may be affected as a response to the cyanophage presence.

Results

Response of cyanobacterial strains to cyanophage additions

The possible impact of Ma-LMM01 and Cr-LKS4 on different strains of two cyanobacterial species (*M. aeruginosa* and *R. raciborskii*) has been investigated by the monitoring of several physiological parameters: OD_{730}nm (Table S1), cell number, Fv/Fm (maximum quantum yield of PSII), toxin content (microcystin or cylindrospermopsin)

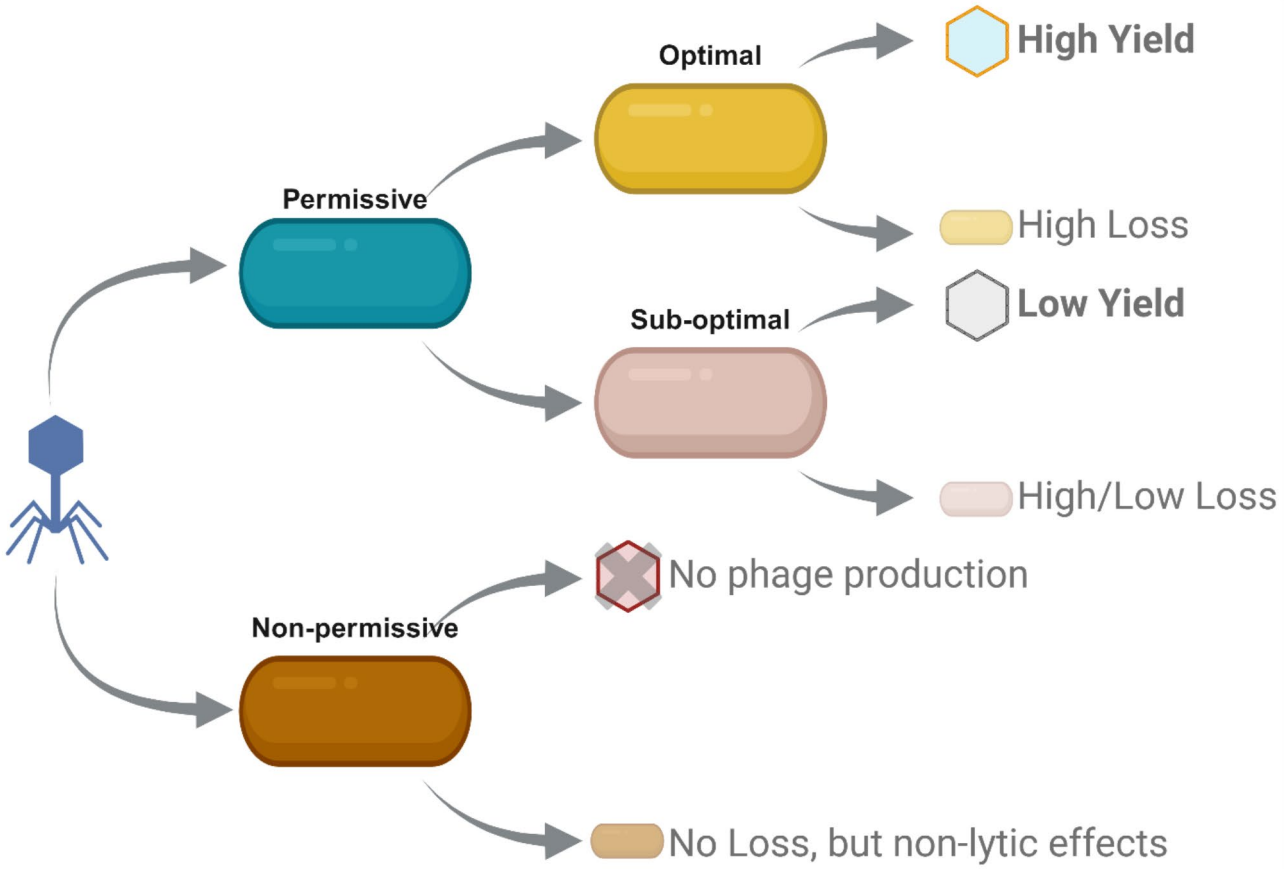

Fig. 1. Conceptual framework of this study. Phage potentially can attempt to infect either permissive or non-permissive host. In the latter case, no phage production occurs as infection is inhibited due to various reasons (e.g. resistance). In case of permissive host, phage can either infect its optimal host (e.g. characterized by relatively better absorption, shorter latent period and higher burst size) which leads to the high final phage yield, or sub-optimal host, leading to lower final yield. Reversion of host (non-) permissiveness or alterations in host compatibility for phage replication are possible due to mutations, selection, and changes in growth or environmental conditions.

and expression of toxin-producing genes (*mcy* or *cyr* cluster). Furthermore, virus titer and the occurrence of lysis has also been presented in order to summarize all relevant findings (Table 1).

Cyanophage dynamics and viral yields

The infection dynamics and changes in cyanophage titer over the time of incubation experiments of Cr-LKS4 infecting its original (optimal) host *R. raciborskii* strain KLL07 and of Ma-LMM01 infecting its original (optimal) host *M. aeruginosa* strain NIES-298 were in general similar to those observed in previous studies[50], showing a drastic increase in their titers at the end of their predicted latent period (Fig. 2). No phage production was observed for other strains, except for PCC 7813 inoculated with Cr-LKS4. Although the increase at 48 h post infection (hpi) was not statistically significant (Fig. 2C), around 50% enhanced phage titer of CrLKS4 in 4 of 5 biological replicates has been observed (Table S1). For other virus-host pairs, the titer of initially added phages decreased over the course of incubation experiment (Fig. 2, Fig. S1, Table S1).

Comparison of the adsorption plots (Fig. 3a, Table S1) shows slow (reduced titre in the filtered fraction between 18 and 21 hpi) and yet still moderately efficient adsorption of Cr-LKS4 (67% of phage adsorbed) to its optimal host strain *R. raciborskii* KLL07. The adsorption efficiency in the PCC 7813 culture could not be determined due to the lack of significant differences in phage titer between different time points over period of 24 h (Fig. 3a).

The timing of host lysis, measured as elevated phage titer, was also different (Fig. 3b). Phage titer started increasing much earlier (at 72 hpi) in the optimal host *R. raciborskii* strain KLL07 compared to the sub-optimal host *M. aeruginosa* PCC 7813 (at 168 hpi). The efficiency of phage multiplication was dramatically higher in the KLL07 culture (approx. 1146-fold increase at the end of the experiment), than in PCC 7813 (approx. 2.5-fold increase) indicating a dramatically lower infection efficiency of Cr-LKS4 in this sub-optimal host (Fig. 3b). Such poor and inconsistent phage adsorption (Fig. 3a) suggests asynchronous infections, which may result from

Phage	Parameter	Host (cyanobacterial strain)				
		M. aeruginosa NIES-298	*M. aeruginosa* PCC 7813	*R. raciborskii* KLL07	*R. raciborskii* CS-505	*R. raciborskii* CS-506
Ma-LMM01	Phage production	✓				
	Lysis	✓				
	Growth	✓(↓)				✓(↓)
	Photosynthesis	✓(↓)			✓(↑)	✓(↓)
	Toxin production	I (↓) E (↓)				
	Gene expression					
Cr-LKS4	Phage production		✓	✓		
	Lysis		✓	✓		
	Growth	✓(↓)	✓(↓)	✓(↓)		✓(↓)
	Photosynthesis	✓(↓)	✓(↓)	✓(↓)		
	Toxin production	I (↑) E (↓)				I (↑)
	Gene expression					

Table 1. The effect of Cr-LKS4 and Ma-LMM01 phages on different cyanobacterial hosts. *M. Aeruginosa* NIES-298 is the optimal host of Ma-LMM01 (marked in blue) whereas *R. Raciborskii* KLL07 is the optimal host of Cr-LKS4 (marked in orange). "✓" indicates observed alteration (increase (↑) or decrease (↓)) of the measured parameter in comparison to control (non-infected) culture. Letters indicate intracellular (I) or extracellular (E) toxin level.

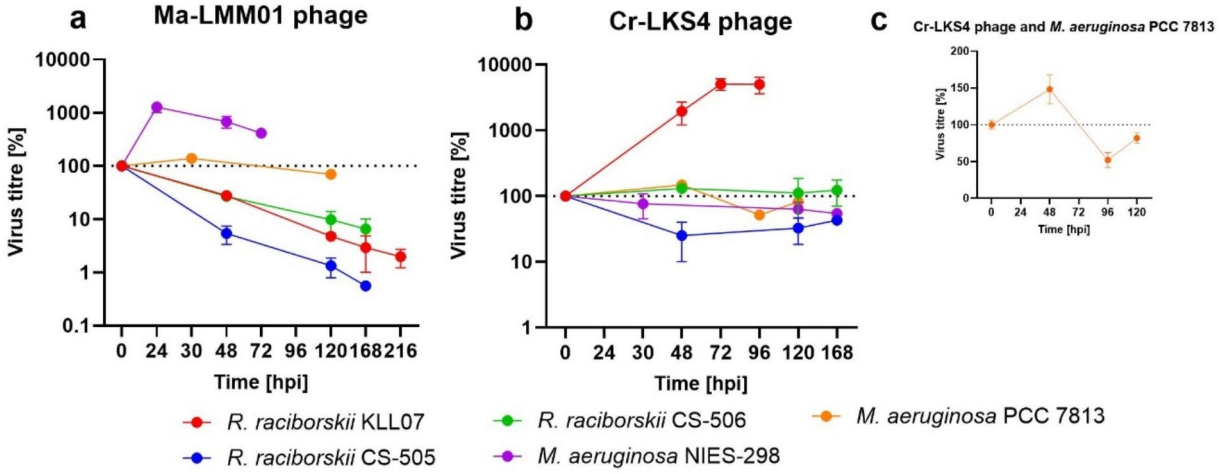

Fig. 2. Changes in virus titer normalized to timepoint 0 (100%) in cultures infected with: Ma-LMM01 (a) or Cr-LKS4 phage (b, c). The length of the experiment varied for each strain-phage pair. Additional internal plot (c) shows smaller but statistically important increase of the Cr-LKS4 titre during *M. aeruginosa* PCC 7813 infection.

significant variation in the physiological state of individual cells within the filaments or the loss of cyanophage infectivity under the given medium conditions.

Growth alterations in response to cyanophage additions

The dynamics of cell abundance of cultures inoculated with phages, which reflects the sum of the growth and cell lysis, were affected in most of the tested strains (Fig. 4, Fig. S2, Table S1). Significant decrease of cell numbers ($p < 0.001$) of *M. aeruginosa* NIES-298 culture infected by phage Ma-LMM01, *R. raciborskii* KLL07 culture infected by Cr-LKS4, and *M. aeruginosa* PCC 7813 culture infected by Cr-LKS4 accompanied with the increased phage titers has been observed (Fig. 2), and therefore, can be attributed to virus-induced cell lysis. We observed significant inhibition of culture growth for most of the other tested strains, with the changes in cyanobacteria cell numbers specific for each strain and phage inoculum (Fig. S2). Only in the case of *M. aeruginosa* PCC 7813, the regrowth of the culture within the timeframe of our incubations was observed (Fig. S2b). In the remaining strains and aforementioned phages, growth was not affected (Fig. S2). The cell number of cultures with active phage normalized to timpoint 0 (Fig. 4) indicated that the Ma-LMM01 phage may affect negatively the abundance of the population of its optimal host (*M. aeruginosa* NIES-298) and also, in longer perspective, the population of

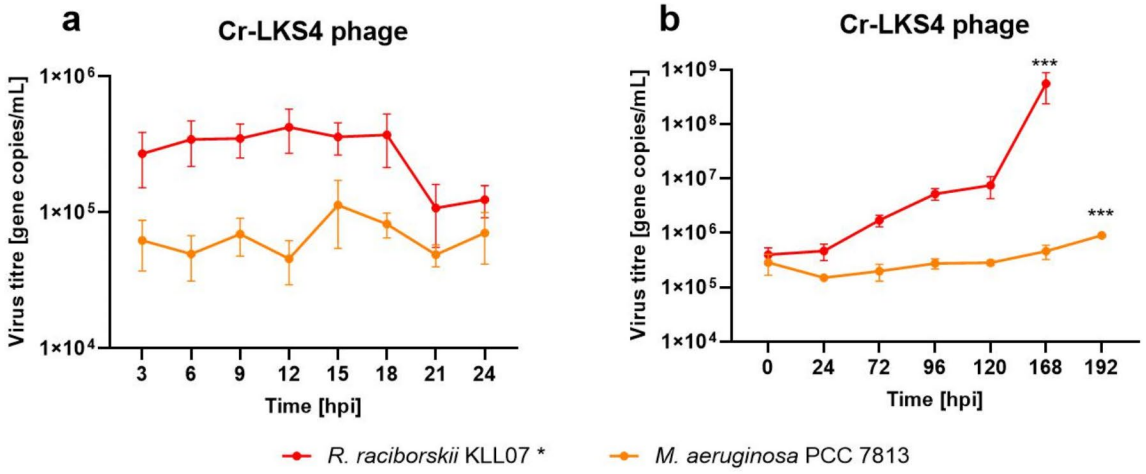

Fig. 3. The viral titre in filtered fraction (measuring free phage particles thus adsorption process) at 24 hpi (a) and the total number of phage DNA copies at the end of infection of *R. raciborskii* KLL07 and PCC 7813 with Cr-LKS4 (MOI 0.01) (b). Asterix (*) indicates optimal host of the tested phage. Statistically significant differences in comparison to the initial values have been indicated by *** $p < 0.001$.

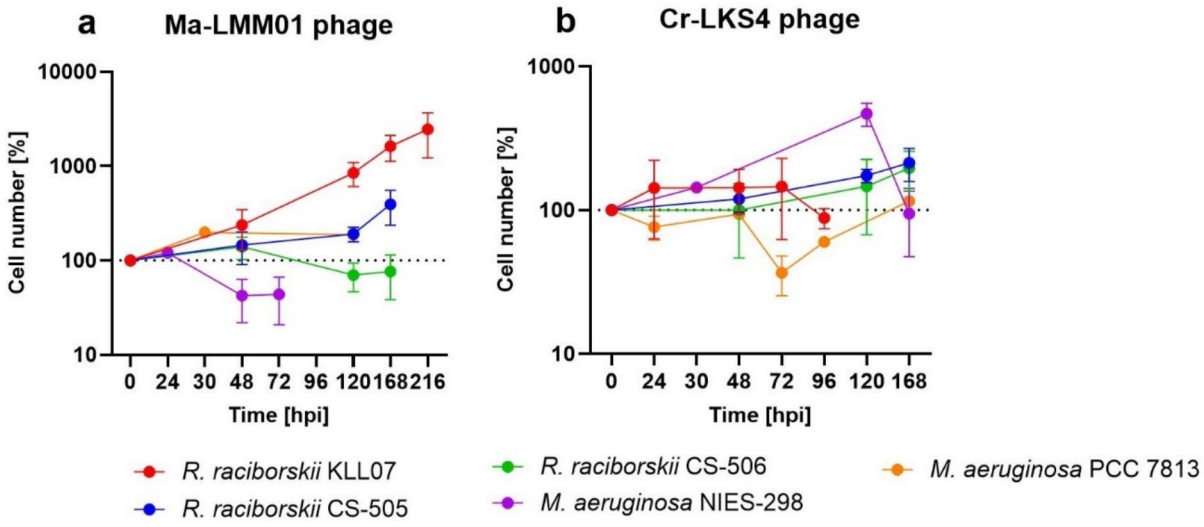

Fig. 4. Cell number normalized to timepoint 0 (100%) in the cultures of *M. aeruginosa* and *R. raciborskii* inoculated with Ma-LMM01 (a) or Cr-LKS4 phage (b). The length of the experiment varied for each strain-phage pair.

R. raciborskii CS-506 whereas the Cr-LKS4 phage reduced the abundance of *R. raciborskii* KLL07 (optimal host) but also both *M. aeruginosa* strains.

Photosynthetic activity

Maximal performance of PSII expressed by Fv/Fm ratio (see Methods) reflects an overall photosynthetic efficiency of cyanobacteria and can be influenced by different (external and internal) stress factors. Altered Fv/Fm observed in the infected cultures are presented in Fig. 5a, b (see also Fig. S3 and Table S1). A dramatic decrease of Fv/Fm occurred already after 24 hpi ($p < 0.001$) in NIES-298 infected by Ma-LMM01 (Fig. 5a), whereas in *R. raciborskii* CS-506 culture the Fv/Fm was stable at least until 48 hpi, and dropped significantly at 120 and 168 hpi ($p < 0.001$, Fig. 5). Interestingly, *R. raciborskii* CS-505 reacted to the presence of Ma-LMM01

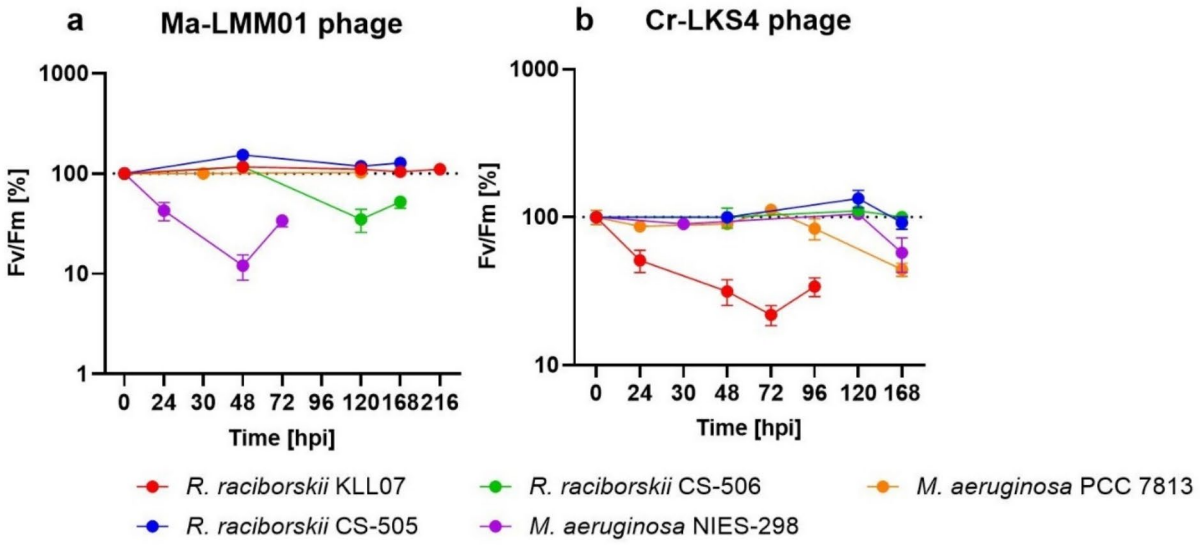

Fig. 5. Changes in overall photosynthetic performance (Fv/Fm) normalized to control at each timepoint (100%) in the cultures of *M. aeruginosa* and *R. raciborskii* inoculated with Ma-LMM01 (a) or Cr-LKS4 phage (b). The length of the experiment varied for each strain-phage pair.

by increasing its photosynthetic performance ($p < 0.001$, Fig. 5 and Fig.S3) Photosynthetic performance was also affected negatively by Cr-LKS4 phage in three other strains (KLL07, NIES-298 and PCC 7813, $p < 0.001$); in KLL07 the Fv/Fm ratio was reduced directly after infection and was on the same low level until the end of infection cycle (Fig. 5b). *M aeruginosa* strains reacted differently to the presence of Cr-LKS4 phage: Fv/Fm ratio of both PCC 7813 and NIES-298 strains was stable (the same as in control) up to 72 or 120 hpi, respectively, and decreased significantly ($p < 0.001$) only at 120 or 168 hpi (Fig. 5b). No changes at this significance level ($p < 0.001$) in PSII activity were observed for the remaining strains after phage inoculation (Fig. S3, Table S1).

Toxicity

Addition of cyanophages induced alterations in both the concentration of intracellular cyanotoxin levels and the expression of genes encoding these toxins in several *R. raciborskii* and *M. aeruginosa* strains tested in this study (Table S1). The infection of *M. aeruginosa* NIES-298 by Ma-LMM01 phage resulted in the significant drop ($p < 0.001$) of intracellular toxin level of the culture, as a consequence of growth inhibition and cell lysis (Fig. 6a). The cellular MC quota (ng/cell) also decreased and was 5-fold lower ($p < 0.05$) compared to the control treatment at the 120 hpi (Fig. 6a), while extracellular content of MC was below the detection limit (Fig. S4). No statistically significant changes in the intra- and extracellular MC concentration were found in *M. aeruginosa* strain PCC 7813 after addition of cyanophage Ma-LMM01 (Fig. 6b), (Fig. S4). The exposure of MC-producing strains (*M. aeruginosa* NIES-298 and PCC 7813) to the Cr-LKS4 cyanophage have also caused a different response. In the *M. aeruginosa* NIES-298 culture we observed the reduced total concentration of intracellular ($p < 0.001$) MC level (mg/mL), while cellular MC quota increased at 168 hpi ($p < 0.05$), indicating higher MC production and elevated toxicity of the remaining non-infected cells (Fig. 6c, Fig. S4). In the case of *M. aeruginosa* strain PCC 7813, neither the intracellular MC level nor the cellular MC quota differed from the control cultures, but the elevated extracellular MC level was observed at 120 hpi ($p < 0.05$), which suggests the higher MC excretion induced after phage inoculation (Fig. 6d, Fig. S4).

The response of CYN-producing *R. raciborskii* differed between the strains tested and cyanophage inoculums. The addition of cyanophage Ma-LMM01 did not alter the cellular CYN quota neither in CS-505 nor CS-506 (Fig. 6e, f), although the total concentration of intracellular toxins was lower in comparison to the control culture of *R. raciborskii* CS-506 at 168 hpi ($p < 0.001$), which may reflect the growth inhibition (see Fig. 6f). In the presence of the Cr-LKS4 cyanophage, the total intracellular CYN level was stable compared to their respective controls (Fig. 6d). However, the average CYN cell quota increased in the culture of *R. raciborskii* CS-506, although due to very high variation at t0, this change was not statistically significant (Fig. 6h), while it remained unchanged in *R. raciborskii* CS-505 (Fig. 6g).

The relative expression of toxin-producing genes in 4 toxic strains was highly variable through time and differed between all cyanophage-cyanobacteria pairs in terms of their dynamics and the overall magnitude of change (Fig. 7, Table S1). The expression of *mcyB* gene was temporarily upregulated at 30 hpi in the optimal host (*M. aeruginosa* NIES-298) infected by Ma-LMM01 which coincided with the lysis of this culture (Figs. 2 and 4) whereas the level of *mcyE* transcripts remained unchanged (Fig. 7a). In the culture of *M. aeruginosa* PCC 7813 (non-permissive host for Ma-LMM01), both genes (*mcyB* and *mcyE*) were continuously upregulated compared

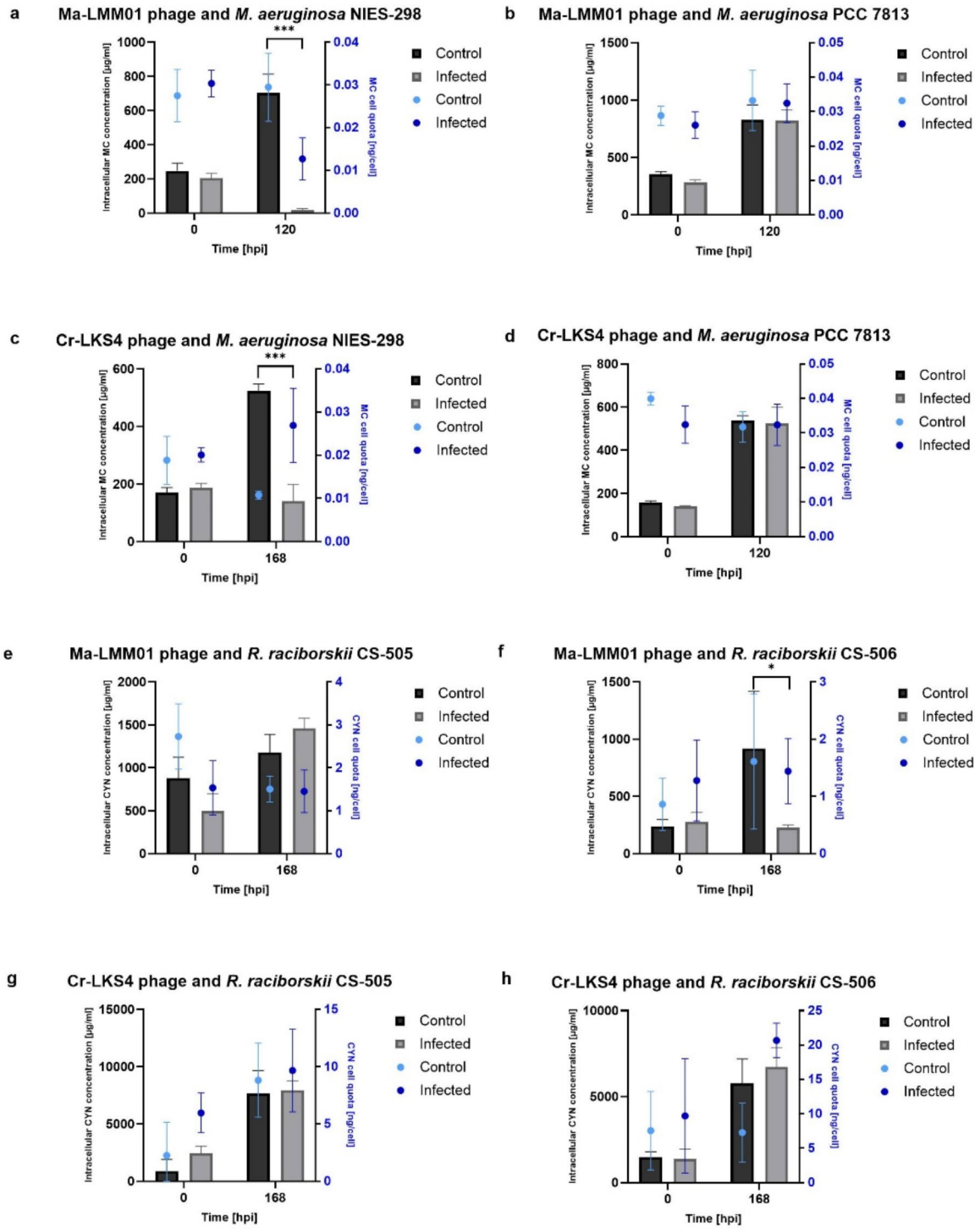

Fig. 6. Microcystin (MC) and cylindrospermopsin (CYN) level in the control and infected cultures of *M. aeruginosa* (Fig. 6a-d) and *R. raciborskii* strains (Fig. 6e-h). Grey blocks show the intracellular level expressed in µg of toxin per mL of culture, whereas blue circles indicate MC or CYN cell quota (ng/cell). (a) Ma-LMM01 vs. NIES-298; (b) Ma-LMM01 vs. PCC 7813; (c) Cr-LKS4 vs. NIES-298; (d) Cr-LKS4 vs. PCC 7813; (e) Ma-LMM01 vs. CS-505; (f) Ma-LMM01 vs. CS-506; (g) Cr-LKS4 vs. CS-505; (h) Cr-LKS4 vs. CS-506. Mean ± SD are shown. Statistically significant difference between control and experimental group at the end of the experiment has been indicated by * $p < 0.05$, ** $p < 0.01$, *** $p < 0.001$.

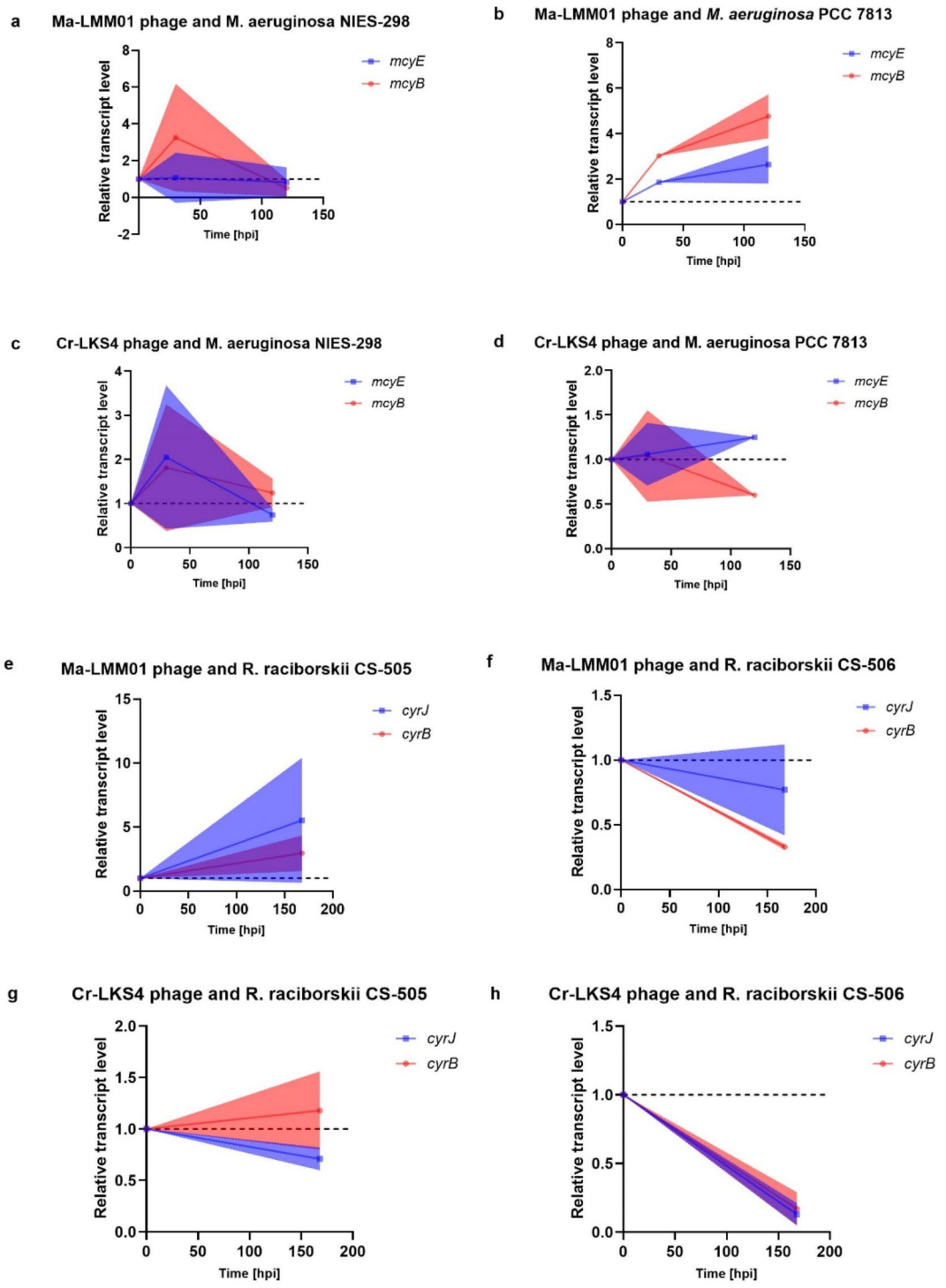

Fig. 7. Gene expression level of toxin-encoding genes (*mcy* or *cyr*) in response to cyanophage inoculation in *M. aeruginosa* and *R. raciborskii* cultures in relation to control (non-infected group). Blue colour was used to show *mcyE* and *cyrJ* transcript levels while red indicates *mcyB* and *cyrB*. Data from the beginning of the experiment (0 hpi) and after 120 or 168 hpi. (a) Ma-LMM01 vs. NIES-298; (b) Ma-LMM01 vs. PCC 7813; (c) Cr-LKS4 vs. NIES-298; (d) Cr-LKS4 vs. PCC 7813; (e) Ma-LMM01 vs. CS-505; (f) Ma-LMM01 vs. CS-506; (g) Cr-LKS4 vs. CS-505; (h) Cr-LKS4 vs. CS-506. Mean (circles) ± SD (shaded area) are shown.

to the control cultures throughout the entire experiment (Fig. 7B). When *M. aeruginosa* strain NIES-298 was infected by cyanophage Cr-LKS4, both genes were temporarily upregulated (at 30 hpi) (Fig. 7c). Inoculation of cyanophage Cr-LKS4 with the *M. aeruginosa* strain PCC 7813 led to the downregulation of the expression of *mcyB*, while the transcript levels of *mcyE* remained unchanged (Fig. 7d). In the case of *R. raciborskii* CS-505, the transcript abundance of analyzed CYN encoding genes increased compared to the control treatments after addition of cyanophage Ma-LMM01 (Fig. 7e), while remained unchanged if inoculated with Cr-LKS4 cyanophage (Fig. 7g). The expression of *cyrJ* and *cyrB* genes was downregulated after exposure of *R. raciborskii* CS-506 to both phages, but to a higher extent in the presence of Cr-LKS4 (Fig. 7f, h).

Discussion

In this study, we attempted to characterize the infection parameters of two different cyanophages across optimal, sub-optimal, and non-permissive hosts. We also examined how additions of cyanophages affect the dynamics of permissive and non-permissive host populations in experimental culture incubations. Our findings indicate that: (i) cross-infectivity might reduce the success of cyanophage under conditions of high-density of sub-optimal host; and (ii) the effects of cyanophage addition on the physiological parameters of cyanobacteria vary significantly depending on the combination of a virus and host strain. Altogether, results show that even a small subset of cyanophages and cyanobacteria combinations as tested in this study resulted in multiple different outcomes, suggesting high variability in viral effect on community dynamics. Therefore, we suggest that this outcome primarily depends on the presence and relative abundance of sub-optimal and non-permissive hosts in the environment, as well as on the exact level of viral effect on the specific hosts in this environment, as this may vary in natural populations. These observations in the context of cyanophage and cyanobacteria population interactions, community dynamics, and implications for ecosystem health and bloom toxicity will be discussed in the next sections.

The success of a virus, in terms of abundance, leading to its impact on the host and functioning of a microbial system is determined by virus production, its loss, and the contact rate with the host[51]. The existing ecological models [e.g. 29] in most cases simplify virus-host dynamics to a single pairwise interactions where one virus infects only one host either at species or strain level[52]. Under such a scenario, higher host densities and growth rate increase the likelihood of successful cyanophage infection, leading to dynamic and cyclic changes in cyanophage and bacterial abundance as would be expected for Lotka-Volterra predator-prey relationships[53]. In addition, it has been shown that lysis timing, beside other factors such genetic similarity, molecular regulation, multiplicity of infection or host and environmental conditions among others, might also depend on host density, and thus earlier lysis might be favored under dense host conditions and delayed when hosts are sparse[54,55]. However, in complex food webs consisting of diverse host populations and communities and where viruses can cross-infect multiple hosts, the production of a single cyanophage genotype would be a sum of new virions yielded in all permissive hosts emerging across the gradient of virus-host compatibility (from optimal to low compatibility;[56]). It would, therefore, likely be subject to significant variation in adsorption, latent period, lysis time and burst size owing to host compatibility differences in conjunction with changes in host density and continuous evolutionary shifts. The highly dynamic nature of host susceptibility to a phage owing to mutations and selection (which were not studied in this work), would add the temporal dimension to co-occurring interactions and viral effects. However, this study shows that contrary to a single virus-host pair interactions, efficiency of infection (in terms of virion yield and lysis timing) would be reduced as the number of permissive, yet sub-optimal hosts increase[34,57]. Cyanophage yield was significantly lower in our incubations when infecting sub-optimal host (Fig. 2), which agrees with current nested infection network models[58] and experimental studies[59].

From the perspective of a single virus dynamics (abundance and distribution), the ability of a cyanophage to infect several different strains (e.g., Cr-LKS4; see above) represents a beneficial adaptation, ensuring virus survival and transmission under conditions of low densities of permissible hosts[60]. However, when the population density of all permissible hosts is high, as tested in this study, cyanophages may attach to or attempt to infect less suitable (sub-optimal) hosts, only to fail or produce very low yields[61], as observed for Cr-LKS4 in PCC 7813 (Fig. 3b). This suggests that increased attachment to sub-optimal hosts (e.g., during bloom conditions with higher host densities) could act as a net sink for cyanophages (Figs. 2c and 3b). Consequently, fewer viruses released from sub-optimal hosts would reduce not only the transmission rate but, more importantly, the number of new successful infections. As discussed above, this would diminish the overall impact of cyanophages on the population and community. One might also expect that high host availability could allow cyanophages to temporarily overcome dispersal barriers and successfully colonize an entire bloom population, as demonstrated by *Microcystis*[44]. Here, however, we propose that the increased presence of permissive but sub-optimal hosts could restrict cyanophage spread across the cyanobacterial population or community. Counterintuitively, this implies that dispersal limitations can persist even at high host densities, significantly shaping cyanophage distribution and virus-host interactions. The extent of this limitation, on the other hand, would depend on the adsorption level of cyanophage population to the sub-optimal host. Low or reversible adsorption may thus alleviate the negative effect of the sub-optimal host on cyanophage dynamics and distribution. The results of our study highlight the complex interplay between phage adsorption (Fig. 3a), lysis timing (Fig. 3b), and virion production (final yield at the end of the experiment, Fig. 2) on the success of a cyanophage under conditions of optimal and sub-optimal hosts.

Differences in adsorption can be related to the structure of surface receptors making it more difficult for cyanophages to attach and successfully infect sub-optimal hosts[1,62]. In addition, various defense mechanisms of the host (e.g. abortive infection, sporulation, etc.) can lead to fewer virions produced per infection cycle[2]. Indeed, in *Microcystis aeruginosa* one of the largest numbers of putative antiviral defence genes of all prokaryotic or archaeal species has been found[63]. In addition, sub-optimal hosts may lack the appropriate cellular machinery or resources necessary for efficient viral replication and lysis processes, potentially leading to longer replication

cycles[64]. This would thus reduce the overall viral yield compared to what would be achieved with optimal hosts[65] limiting the spread of the virus to other permissive hosts. Altogether, our data imply that controlling effect of cyanophages on the blooms depends strongly on the structure of the cyanobacterial community as a whole, and that viruses and their hosts might co-occur at high abundances[27,56,66], such as those during freshwater cyanobacterial blooms, owing to balancing effect of sub-optimal host. Furthermore, different processed, not verified here, may influence virus-host interaction in natural environment, e.g. formation of colonies, which is thought to have a significant effect on phage infection and spread or vertical migration by gas vesicles that may also have an effect on the host cell availability.

From the perspective of host population and bloom dynamics, our results suggest that shared infections as well as non-lytic effects could have substantial roles in shaping cyanobacterial communities adding to the existing variability in their growth, activity (e.g. PSII) and toxin production (Figs. 6 and 7). This in turn might reduce our ability to predict the composition and dynamics of cyanobacterial community during intensive summer blooms. In natural environments, two cyanobacteria genotypes or species co-occurring at the same time in close spatial proximity are likely to be involved in direct intra-/inter-species competition for available resources[67], which inherently implies a negative direction in the relationship between the abundances of two competing taxa (competitive exclusion principle). Higher population densities of competing members within the community would strengthen both competitive interactions and density-dependent interactions with the predators. Shared infections accompanied by unequal cyanophage effects (Figs. 4 and 5) can alter competitive abilities and strength of interactions between competing hosts either by increasing or decreasing the slope of negative relationship. For example, in case when optimal host is also a better competitor for available resources, shared infections would reduce the strength of competition (elimination of competitive exclusion) between the two taxa[29]. If the optimal host is also a worse competitor, then this could result in local extinction event in turn creating favorable conditions leading to the blooms dominated by a single genotype or clonal population[68,69].

This study, in addition to commonly observed lytic effects of cyanophages, also demonstrates that viruses can influence co-occurring cyanobacteria community through previously unrecognized non-lytic effects by altering their physiological traits, such as photosynthetic performance, growth rate, toxin production, and population size (Table 1; Figs. 3, 4 and 5). Documented here the phage impact on the basic physiology of the other non-permissive strains that are not infected (lack of phage production) but affected, indicates complex interactions within microbial community. For example, while photosynthetic performance was either unchanged or reduced in many infected cultures, the phage-induced increase of Fv/Fm in *R. raciborskii* CS-505 is worth mentioning. This strain accumulates extremally high level of carotenoids, and myxoxanthophyll in particular[70] which acts as a strong antioxidant. It indicates that observed here non-obvious behavior may reflect the uniqueness of strain's features and a strain-specific response. How these non-lytic effects influence cyanobacteria responses across different species, from individual feature changes to population size, has important implications for understanding how microbial interactions shape communities and affect ecosystems.

The examination of how investigated phages impact toxic cyanobacterial strains in regard to their ability to produce toxins indicated a complex response. During the infection of optimal host *M. aeruginosa* NIES-298, despite the stable or even temporally upregulated expression of *mcy* genes (Fig. 7), a decreased intracellular MC level has been documented (Fig. 5), which suggests that cells that survived the infection had a week metabolic activity (reflected also by a relatively low Fv/Fm, see Fig. 5), and thus a reduced ability to produce toxins. Such an observation indicates that efficient infection induced by Ma-LMM01 phage may cause the significant reduction of MC level in freshwater ecosystems, as a consequence of both lower cell abundance of toxic strains and weakened (at least in short timescale) capability of the toxin production. On the contrary, previous research indicated that when toxic strain *Nodularia spumigena* KAC68 was infected by a lytic cyanophage vB_NodS-kac68v162-1, cellular nodularin (NOD) quota (ng/cell) gradually increased[71]. Therefore, even within optimal cyanobacterial hosts that are efficiently infected, the impact on the toxicity of host cells may be unique and individual strains respond differently. This varied effect reported here can be connected with the documented silent infection of Ma-LMM01[72] which can precisely control the expression of its own genes with no impact on the host transcriptome and thus avoid the activation of host defense systems. The same phage Ma-LMM01 did not lead to any alterations in MC production of non-permissive hosts, neither MC-producing *M. aeruginosa* PCC 7813 nor the CYN-producing CS-505 and CS-506 strains (Fig. 6). On the other hand, the Cr-LKS4 cyanophage modified the toxin production in sub-optimal or non-permissive strains (upregulation of *mcy* genes together with enhanced extracellular MC level in PCC 7813 and cellular MC quota in NIES-298, respectively). These findings may be explained by the putative role of MC in stress (oxidative stress, in particular) underlined in the recent review[73] as MCs have been considered as direct antioxidants[74,75] Furthermore, MCs probably play an essential role in the stress management by specific binding to proteins; such interactions may be important in the adaptation to oxidative stress induced by high light and/or temperature[76]. The deepest physiological analysis and discussion of MC role in oxidative stress management was provided recently by Stark et al.[76] that described the response of MC-producing and non-producing (mutant) *M. aeruginosa* strains to cold. Differential expression of genes involved in the redox balance (glutathione-dependent peroxiredoxin (*pdgx*)) and photosynthetic electron transport chain (cytochrome b559 (*psbE*), cytochrome c oxidase (*coxBAC*)) indicated specific mechanisms of oxidative stress management. Thus, the authors concluded that MC production may substitute some other protective mechanisms against ROS and helps to avoid the stress. Furthermore, it allows allocating efficiently the excitation energy and ensures optimal electron transport thorough photosystems; the later conclusion was supported by photo-physiological measurements. The decreased Fv/Fm ratio in wild type MC-producing strain during acclimation to cold (which was consistent with the putative modulation of pdgx activity by MC) was interpreted as an effective stress management[76]. In this context, our observation (decreased Fv/Fm in both *M. aeruginosa* cultures in later phase of infection by Cr-LKS4 phage, Fig. 4) also suggests that elevated MC accumulation is a cell response to oxidative stress related to phage occurrence. Similarly, although CYN is

considered as a constitutive metabolite whose biosynthesis is correlated to cyanobacterial growth rather than directly to specific environmental conditions [e.g. [77]], we observed that the stress induced by Cr-LKS4 caused the selection of more toxic phenotype of CYN-producing *R. raciborskii* CS-506 strain (reflected by the increased cellular CYN quota).

Our observation indicates that the overall toxicity of MC- or CYN-producing strains depends on the strain response/phage impact. When phage infected and lysed the culture efficiently (LMM01 vs. NIES-298), the MC content was dramatically reduced. The lack of response to cyanophage addition, as observed in PCC 7813 and CS-505 when inoculated with LMM01 (no evidence of non-permissiveness, nor any impact on growth or photosynthetic activity), was also associated with stable MC/CYN production. However, if the phage meets either a sub-optimal host (Cr-LKS4 vs. PCC 7813) or non-permissive (Cr-LKS4 vs. NIES-298 and CS-506), and is able to impact the culture (a growth reduction or/and a decreased photosynthetic efficiency), this type of interaction may have caused the selection of more toxic phenotypes. As suggested by Šulčius et al.[71], the selection for toxic phenotypes could influence interspecies relationships by reducing species loss to predation and enhancing competitive abilities, thereby creating cascading effects throughout the entire food web. The results of this study, however, indicate that cyanophage addition-mediated increased toxicity (Fig. 6), which could presumably confer a competitive advantage to these strains [e.g. [78]], might also come at the expense of growth (Fig. S2), suggesting a growth rate cost of resistance, as reviewed in Avrani et al.[79].

The combined effects of phage infection of optimal and sub-optimal hosts on a cyanobacterial community are still largely unknown. Our results, however, suggest that sharing of the viral predation pressure (e.g. *R. raciborskii* KLL07 and *M. aeruginosa* PCC 7813 infected by cyanophage Cr-LKS4) can have a positive effect on a cyanobacteria community and bloom proliferation as differences in infection efficiencies and yield between different host strains reduce the overall prevalence of a virus and, thus, the probability of new virus infections. This thus also means that shared infections act as a cyanophage sink under high densities of suboptimal hosts. Furthermore, such an individual response in terms of toxin dynamics (production/accumulation), dependent on a strain and a phage type, has important ecological consequences in natural freshwater ecosystems, leading to either reduced or enhanced toxicity of cyanobacterial community and thus impacting the condition of freshwater ecosystems and potentially affecting the health of other organisms within the habitat via trophic interactions.

Materials and methods

Strains and phages

Raphidiopsis raciborskii KLL07 strain and Cr-LKS4 phage were isolated from Lake Kinneret, Israel[80], whereas phage Ma-LMM01 was isolated from Lake Mikata, Japan[50]. *Microcystis aeruginosa* NIES-298 was ordered from NIES Collection and *Microcystis aeruginosa* PCC 7813 from the Pasteur Culture Collection of Cyanobacteria. *Raphidiopsis raciborskii* CS-505 and CS-506 strains were obtained due to the cooperation with A. Willis, CSIRO, Australia. Detailed information on the material is included in Table S1 and S2. Cultures were carried out in CB medium pH 8.0 supplemented with 29,6 nM thiamine, 8,19 nM biotin, 0.738 nM cyanocobalamin and 5.91 nM pyridoxine[81], WC pH 7.4–7.8[82] medium with full nitrogen content (WC100N) and $NaNO_3$ content reduced to 25% (WC25N) or BG-11o medium pH 7,5 with $NaNO_3$[83].

Experimental design

The cultures were maintained under a 14/10-h light-dark cycle with light intensity of 40 µmol m^{-2} s^{-1} and at 20 °C. The cyanophage Ma-LMM01 and Cr-LKS4 inoculum for the incubation experiment was prepared from lysates of *M. aeruginosa* NIES-298 and *R. raciborskii* KLL07, respectively purified using a two-step centrifugation procedure consisting of initial 20-min centrifugation at 2000 x *g* to remove uninfected cells and cell debris, and 60-min centrifugation at 11,000 x *g* to concentrate cyanophages.

The experimental duration and conditions were chosen to match the cyanophage infection cycle. Previous studies have determined the infection cycle duration of Ma-LMM01 to be approximately 24 h[72]. The cyanophage Cr-LKS4 viral cycle time was experimentally found to be around 72–96 h. Hence, samples were collected in different time intervals, depending on the investigated host/phage pair, up to 120 or 168 hpi.

Before the experiment, the fresh unialgal (non-axenic) culture was subdivided into two groups (infected and control treatments), each group had three replicates. These exponentially growing cultures (100 mL each) were preconditioned 1 day in 250 mL Erlenmeyer glass flasks for stabilization. The phage suspension was added to the culture at a volume ratio of 1:20, maintaining a constant ratio while the ratio of added phage particles (gene copies determined by qPCR) to cyanobacterial cells was 10–50, to ensure that all the cells may be infected. In the control group, a heat-inactivated phage suspension was added. Pre-experimental tests confirmed that heat-inactivated phage suspensions had no inhibitory effect on cyanobacterial cultures (data not shown). Samples for the phage titer, growth (OD_{730} nm and cell number), photosystem II activity (PSII), toxin content and expression of genes encoding the toxins were collected at the same time points. Every time the control experiment with a host infected by native phage (NIES-298 with Ma-LMM01 or KLL07 with Cr-LKS4) was carried out simultaneously to verify that phage lysate is active.

Additional infection assays to estimate the adsorption rate of Cr-LKS4 phage were performed for the optimal host *R. raciborskii* KLL07 and the sub-optimal host PCC 7813 with MOI = 0.01. For the original host-pair NIES-298 and Ma-LMM01, this type of assay was performed in previous studies[50]. Six biological replicates were used for each assay. Phage samples were collected to determine the total viral titre (unfiltered samples) and the titre of free, non-attached phage particles (samples filtered through 0.2 µm filters), 100 µL for each fraction. Samples were collected at specific timepoints: 0, 3, 6, 9, 12, 15, 18, 21, 24 hpi. The incubation assays were extended and additional samples at 72, 120, and 168 h were taken to re-examine the duration of the cyanophage life cycle and confirm the production of new virons. The qPCR reactions were prepared by adding 1 µL of DNase (concentration 1 mg/mL) to 9 µL of sample and shortly spinned. Thermocycler protocol consisted of 30 min of

37 °C, 10 min of 95 °C. Afterwards 90 µL of dH2O was added (10x dilution) for the qPCR reaction (described in a paragraph below).

Viral titer

Viral titer was determined by a real-time quantitative polymerase chain reaction (real-time qPCR) by calculating the amount of viral DNA from a standard curve derived from 10-fold dilutions of viral DNA ranging from $1{\cdot}10^5$ to $8.5{\cdot}10^8$ copies of the gene. The primers are listed in Table S3.

For a single qPCR reaction, 4 µL of 10x diluted culture sample, 0.5 µL of each primer pair (10 µM concentration), and 5 µL of 2x concentrated PowerUP SYBR Green Master Mix reaction mixture (Applied Biosystems, catalog number A25742) were used. The temperature profile of the reaction was as follows: UDG activation at 50 °C for 2 min, initial denaturation at 95 °C for 2 min, 40 cycles of amplification at 95 °C for 15 s and 60 °C for 1 min with fluorescence detection after each cycle, followed by a melting curve analysis ranging from 65 °C to 95 °C with a 0.5 °C increment per cycle lasting 5 s, and fluorescence detection after each cycle.

The standard curve was generated based on tenfold dilutions of linearized pJET1.2 plasmid containing target gene fragments. These fragments were obtained by PCR using DreamTaq polymerase (Thermo Scientific, catalog number EP0701) with qPCR primers on genomic DNA template of *M. aeruginosa* NIES-298 and *R. raciborskii* KLL07. The PCR products were then cloned into the pJET1.2 plasmid using the CloneJET PCR Cloning Kit (Thermo Scientific, catalog number K1232). The amplified and purified plasmids were digested with NotI restriction enzyme from the FastDigest kit (Thermo Scientific, catalog number FD0595) to linearize them.

The qPCR primers (Table S3) were designed based on the nucleotide sequences of Cr-LKS4 and Ma-LMM01 viruses, and *M. aeruginosa* and *R. raciborskii* cyanobacteria deposited in the NCBI Nucleotide database. The PrimerQuest Tool, OligoAnalyzer, and Basic Local Alignment Search Tool algorithm were used for primer design.

Cyanobacteria growth

The growth was monitored by the measurement of optical density at 730 nm (OD_{730}) and automatized cell counting (all cells measured, independently on their physiological condition) in a hemocytometer (Bürker chamber). The samples (100 µL of culture) were preserved in formaldehyde solution (5% final concentration) and stored at 4 °C in the dark. The photos of sampled cultures placed in the Bürker chamber were taken using a Genetic Pro (Delta Optical, Poland) light microscope with a camera at five-fold magnification and processed in the ImageJ program (National Institutes of Health) by counting the area covered by cells in each photo. The counted area was converted to the number of cells by a script written in R supported by manual calibration.

Chlorophyll fluorescence

Maximal performance of PSII (Fv/Fm, also described as φ_{P0}) was performed using a Handy PEA + fluorometer with an LPA2 liquid phase adapter (Hansatech Instruments) at saturating exciting light. F0 (ground state chlorophyll fluorescence) and Fm (maximum fluorescence) are measured directly whereas Fv (variable fluorescence) is calculated from the formula Fv = Fm - F0[84].

Toxin measurement

The intracellular microcystin (MC) and cylindrospermopsin (CYN) concentrations were determined using the procedure described by Meriluoto at al[85], with some modifications as follows. The extraction steps required different procedures according to relatively high hydrophobicity of MC and high hydrophily of CYN. Samples of *M. aeruginosa* strains (5 mL) were centrifuged for 5 min, 10,000 x *g* and stored at 20 °C. Supernatant was transferred into new falcons and stored. For intracellular MC extraction, cell pellet was suspended in 1 mL 75% MeOH and cells were disrupted in bath ultrasonicator for 15 min. Then, an ultrasonic disrupter equipped with a microtip probe was used for the further disruption of the cells. Each sample was ultrasonicated for 1 min (1 s sonication, 1 s pause), at 80% power. Samples were kept at 4 °C overnight for better extraction then centrifuged at 10,000 x g for 5 min and supernatants were air-dried overnight. Evaporated extracts were resuspended with 200 µl of 75% MeOH and vortexed. Another centrifugation for 10 min at 10,000 x *g* was applied and 100 µL of supernatant was transferred to the glass vials. Microcystin extraction from medium was performed using SPE cartridges. First, 1 mL of 100% MeOH was added into the frozen samples, and 10 mL of 100% MeOH was used for the conditioning of the cartridges, followed by 10 mL of water. Samples were applied at a flow rate of 10 mL/min. Afterwards, 4 mL of 20% MeOH was added for the washing step and then the cartridges dried completely. Samples were then eluted with 4 mL of acetonitrile containing 0,05% TFA and left for evaporation (air-dried overnight). Evaporated samples were resuspended with 200 µL of 75% MeOH and vortexed. After centrifugation for 10 min at 10,000 x *g*, 100 µL of supernatant was transferred to HPLC vials.

Samples of *R. raciborskii* strains (30 mL) were centrifuged for 10 min, 5000 x *g* at 4 °C and the supernatant was removed. For CYN extraction, the cell pellet was covered with 2 mL 100% MeOH and then put into the bath ultrasonicator for 15 min. Glass beads were added at a ratio of 1:1 (v/v) and samples left for 15 min on a shaker. The samples were then centrifuged at 10,000 x *g* for 10 min and supernatant was air-dried overnight in glass tubes. Evaporated extracts were resuspended with 200 µL of distilled water and centrifuged for 10 min (10000 x *g*) to remove the remaining impurities. The final supernatant was transferred to HPLC vials.

Measurement of the toxin content was carried out using an Agilent 1220 Infinity LC G4294B high performance liquid chromatography system (Agilent Technologies, Inc., USA). HPLC separation was carried out with flow rate 1 mL/min. A mobile phase consisted of: (A) HPLC water + 0,05% trifluoroacetic acid (TFA) and (B) methanol + 0,05% TFA for the CYN determination[86], and (A) HPLC water + 0,05% TFA and (B) ACN + 0,05% TFA for MC[87]. The column oven temperature settled at the 40 °C. Injection volume was 20–40 µL. Standards

used for the toxin identification and concentration determination were MC-LR obtained from the Abo Akademi University (Jussi Meriluoto lab) and CYN isolated from *Anabaena lapponica*[88].

Gene expression

RNAs were collected for the measurement of the *mcy* and *cyr* gene expression. In each of the sampling periods, 4 mL of samples (*M. aeruginosa*) or 15 mL (*R. raciborskii*) was collected into the falcons and 96% EtOH was added to stop transcriptomic activity. Samples were centrifuged for a 5 min at 10,000 x *g*, at 4 °C and pellet was resuspended with 1 mL of supernatant and transferred to the new 2 mL Eppendorf tubes for another centrifugation for 10 min at 10,000 x *g* and 4 °C. Supernatant was discarded and samples stored at -20 °C. During RNA extraction, glass beads were added to cell pellet in 1:1 ratio then 500 µL of TRI reagent and samples were vortexed for 10 min in room temperature then after addition of 100 µL of chloroform vortexed for 15 s. Samples were incubated for 15 min at room temperature then centrifuged for 15 min 10,000 x *g*, at 4 °C. Upper-water phase was taken into new RNase-free tubes, 250 µL of isopropanol was added for the precipitation of the RNA and incubated for 1 h in 4 °C after mixing the tubes gently. Samples were centrifuged again for 20 min at 10,000 x *g*, at 4 °C and supernatant was discarded. For the washing step, 750 µL of 85% RNase-free ethanol was added and centrifuged for 5 min at 10,000 x *g*, at 4 °C. Samples were air-dried and then resuspended with 30 µL of RNase free water and stored at -20 °C.

For cDNA synthesis 0.5 µL of 10x MgCl2 buffer, 4 µL of RNA, 0.5 µL of DNase I (RNase-free Thermo Scientific). RNA was estimated using NanoDrop and approximately 500ng/µL RNA was used. Reaction mixture was incubated for 30 min at 37 °C then DNase was inactivated by adding 0.5 µl of 50nM EDTA and incubated more for 10 min at 65 °C. Afterwards, reaction mixture was created with following elements: 2.1 µL of DEPC-treated water, 1 µL of 10x RT buffer, 0.4 µL of 25x dNTP mix, 1 µL of 10x random primers and 0.5 µL of reverse transcriptase which sums up as 5 µL of mix per sample. Then this mix was combined with 5 µL of RNA treated with DNase I. Specific temperature profile was applied: 10 min at 25 °C, 120 min of 37 °C and 5 min of 85 °C. Prepared samples were stored at 4 °C for further analyses. Synthesized cDNA was analyzed with qPCR using SYBR Green in two replicates using Bio-Rad CFX96 device. Cycles started with 120 s of 50 °C, 120 s of 95 °C, followed by 40 cycles of 95 °C for 15 sand 60 °C for 60 s, and then 65 °C to 95 °C with increment of 0.5 °C temperature increase.

Relative gene expression was interpreted based on the quantification cycle (Cq) value outcomes from qPCR. Housekeeping genes that occur in one copy of the genome, specifically *rpoC* (for *M. aeruginosa*) or *prs/rnpA* (for *R. raciborskii*), were used to normalize transcript abundances while relative quantification was conducted using the ΔΔCt-based method. Changes in the relative expression levels of genes associated with microcystin (*mcyE*, *mcyB*), or cylindrospermopsin (*cyrJ*, *cyrB*) production during the cyanophage infection were calculated (Table S1).

Statistical analyses

While performing statistical analyses and creating graphs, GraphPrism software for Windows was used. One-way ANOVA test was performed with Tukey's *post-hoc* test in Statistica. Missing and inaccurate values were not included in the statistical analysis. There were three replicates in each control and experimental group in every timepoint. Values in the graphs indicate the mean number of the three replicates for each group at specific timepoint, error bars in the graphs show the standard deviation of the means (SD). Graphs were prepared and presented in GraphPrism software. Mean differences with a significance value lower than $^{*}p < 0.05$, $^{**}p < 0.01$, $^{***}p < 0.001$, were considered statistically significant.

Data availability

All data generated or analysed during this study are included in this published article (and its Supplementary Information files).

Received: 23 September 2024; Accepted: 21 January 2025
Published online: 24 January 2025

References

1. Suttle, C. A. Viruses in the sea. *Nature* **437**, 356–361 (2005).
2. Grasso, C. R. et al. A review of cyanophage–host relationships: highlighting cyanophages as a potential cyanobacteria control strategy. *Toxins* **14**, 385 (2022).
3. Gregory, A. C. et al. Genomic differentiation among wild cyanophages despite widespread horizontal gene transfer. *BMC Genom.* **17**, 1–13 (2016).
4. Mole, R., Meredith, D. & Adams, D. G. Growth and phage resistance of *Anabaena* sp. strain PCC 7120 in the presence of cyanophage AN-15. *J. Appl. Phycol.* **9**, 339–345 (1997).
5. Thompson, L. R. et al. Phage auxiliary metabolic genes and the redirection of cyanobacterial host carbon metabolism. *Proc. Natl. Acad. Sci.* **108**, E757–E764. https://doi.org/10.1073/pnas.110216410 (2011).
6. Puxty, R. J., Millard, A. D., Evans, D. J. & Scanlan, D. J. Shedding new light on viral photosynthesis. *Photosynth Res.* **126**, 71–97 (2015).
7. Zeng, Q. & Chisholm, S. W. Marine viruses exploit their host's two-component regulatory system in response to resource limitation. *Curr. Biol.* **22**, 124–128 (2012).
8. Cairns, J., Coloma, S., Sivonen, K. & Hiltunen, T. Evolving interactions between diazotrophic cyanobacterium and phage mediate nitrogen release and host competitive ability. *Roy Soc. Open. Sci.* **3**, 160839. https://doi.org/10.1098/rsos.160839 (2016).
9. Coloma, S. E. et al. Newly isolated *Nodularia* phage influences cyanobacterial community dynamics. *Environ. Microbiol.* **19**, 273–286 (2017).
10. Shelford, E. J., Middelboe, M., Møller, E. F. & Suttle, C. A. Virus-driven nitrogen cycling enhances phytoplankton growth. *Aquat. Microb. Ecol.* **66**, 41–46 (2012).

11. Sun, Y. et al. Genetic diversity and co-occurrence patterns of marine cyanopodoviruses and picocyanobacteria. *Appl. Environ. Microb.* **84**, e00591–e00518. 10.1128/AEM.00591-18 (2018).
12. Dart, E., Fuhrman, J. A. & Ahlgren, N. A. Diverse marine T4-like cyanophage communities are primarily comprised of low-abundance species including species with distinct seasonal, persistent, occasional, or sporadic dynamics. *Viruses* **15**, 581 (2023).
13. Levin, B. R. & Bull, J. J. Population and evolutionary dynamics of phage therapy. *Nat. Rev. Microbiol.* **2**, 166–173 (2004).
14. Knowles, B. et al. Lytic to temperate switching of viral communities. *Nature* **531**, 466–470. https://doi.org/10.1038/nature17193 (2016).
15. Koskella, B. & Meaden, S. Understanding bacteriophage specificity in natural microbial communities. *Viruses* **5**, 806–823. https://doi.org/10.3390/v5030806 (2013).
16. Holmfeldt, K. et al. Large-scale maps of variable infection efficiencies in aquatic Bacteroidetes phage-host model systems. *Environ. Microbiol.* **18**, 3949–3961 (2016).
17. Koskella, B. & Brockhurst, M. A. Bacteria-phage coevolution as a driver of ecological and evolutionary processes in microbial communities. *FEMS Microbiol. Rev.* **38**, 916–931 (2014).
18. Johnson, D. W. & Potts, M. Host range of LPP cyanophages. *Int. J. Syst. Bacteriol.* **35**, 76–78 (1985).
19. Wichels, A. et al. Bacteriophage diversity in the North Sea. *Appl. Environ. Microbiol.* **64**, 4128–4133 (1998).
20. Holmfeldt, K., Middelboe, M., Nybroe, O. & Riemann, L. Large variabilities in host strain susceptibility and phage host range govern interactions between lytic marine phages and their *Flavobacterium* hosts. *Appl. Environ. Microbiol.* **73**, 6730–6739 (2007).
21. Safferman, R. S. & Morris, M. E. Observations on the occurrence, distribution, and seasonal incidence of blue-green algal viruses. *Appl. Microbiol.* **15**, 1219–1222 (1967).
22. Sullivan, M. B., Waterbury, J. B. & Chisholm, S. W. Cyanophages infecting the oceanic cyanobacterium *Prochlorococcus*. *Nature* 424, 1047–1051. Erratum in: *Nature* 426, 584 (2003).
23. Pollard, P. C. & Young, L. M. Lake viruses lyse cyanobacteria, *Cylindrospermopsis raciborskii*, enhances filamentous-host dispersal in Australia. *Acta Oecol.* **36**, 114–119 (2010).
24. Watkins, S. C., Smith, J. R., Hayes, P. K. & Watts, J. E. M. Characterisation of host growth after infection with a broad-range freshwater cyanopodophage. *PLOS One*. **9**, e87339. https://doi.org/10.1371/journal.pone.0087339 (2014).
25. Stough, J. M. et al. Molecular prediction of lytic vs lysogenic states for Microcystis phage: metatranscriptomic evidence of lysogeny during large bloom events. *PLoS One*. **12** (9), e0184146 (2017).
26. Pound, H. L. & Wilhelm, S. W. Tracing the active genetic diversity of Microcystis and Microcystis phage through a temporal survey of Taihu. *PLoS One*. **15** (12), e0244482. https://doi.org/10.1371/journal.pone.0244482 (2020).
27. Flores, C. O., Valverde, S. & Weitz, J. S. Multi-scale structure and geographic drivers of cross-infection within marine bacteria and phages. *ISME J.* **7**, 520–532 (2013).
28. Brum, J. R., Hurwitz, B. L., Schofield, O., Ducklow, H. W. & Sullivan, M. B. Seasonal time bombs: dominant temperate viruses affect Southern Ocean microbial dynamics. *ISME J.* **10** (2), 437–449 (2016).
29. Thingstad, T. F. Elements of a theory for the mechanisms controlling abundance, diversity, and biogeochemical role of lytic bacterial viruses in aquatic systems. *Limnol. Oceanogr.* **45**, 1320–1328 (2000).
30. Avrani, S., Wurtzel, O., Sharon, I., Sorek, R. & Lindell, D. Genomic island variability facilitates Prochlorococcus–virus coexistence. *Nature* **474**, 604–608. https://doi.org/10.1038/nature10172 (2011).
31. Mann, N. H., Clokie, M. R. J. Cyanophages in *In Ecology of Cyanobacteria II*. (ed Whitton, B.) 535–557 (Springer, 2012).
32. de Melo, A. C. C. et al. Characterization of a bacteriophage with broad host range against strains of *Pseudomonas aeruginosa* isolated from domestic animals. *BMC Microbiol.* **19**, 1–15 (2019).
33. Holtappels, D., Alfenas-Zerbini, P. & Koskella, B. Drivers and consequences of bacteriophage host range. *FEMS Microbiol. Rev.* **47**, 1–10 (2023).
34. Jover, L. F., Cortez, M. H. & Weitz, J. S. Mechanisms of multi-strain coexistence in host-phage systems with nested infection networks. *J. Theor. Biol.* **332**, 65–77 (2013).
35. de Jonge, P. A., Nobrega, F. L., Brouns, S. J. J. & Dutilh, B. E. Molecular and evolutionary determinants of bacteriophage host range. *Trends Microbiol.* **27**, 51–63 (2019).
36. Wang, J. et al. Interaction between cyanophage MaMV-DC and eight *Microcystis* strains, revealed by genetic defense systems. *Harmful Algae*. **85**, 101699. https://doi.org/10.1016/j.hal.2019.101699 (2019).
37. Stern, A. & Sorek, R. The phage-host arms race: shaping the evolution of microbes. *Bioessays* **33** (1), 43–51 (2011).
38. Schwartz, D. A. & Lindell, D. Genetic hurdles limit the arms race between Prochlorococcus and the T7-like podoviruses infecting them. *ISME J.* **11** (8), 1836–1851 (2017).
39. Hampton, H. G., Watson, B. N. & Fineran, P. C. The arms race between bacteria and their phage foes. *Nature* **577** (7790), 327–336 (2020).
40. Morimoto, D., Šulčius, S. & Yoshida, T. Viruses of freshwater bloom-forming cyanobacteria: genomic features, infection strategies and coexistence with the host. *Env Microbiol. Rep.* **12** (5), 486–502 (2020).
41. Coulombe, A. M. & Robinson, G. G. C. Collapsing *Aphanizomenon Flos-Aquae* blooms: possible contributions of photo-oxidation, O2 toxicity, and cyanophages. *Can. J. Bot.* **59**, 1277–1284 (1981).
42. Manage, P. M., Kawabata, Z. & Nakano, S. Seasonal changes in densities of cyanophage infectious to *Microcystis aeruginosa* in a hypereutrophic pond. *Hydrobiologia* **411**, 211–216 (1999).
43. Simis, S. G., Tijdens, M., Hoogveld, H. L. & Gons, H. J. Optical changes associated with cyanobacterial bloom termination by viral lysis. *J. Plankton Res.* **27** (9), 937–949 (2005).
44. Steffen, M. M. et al. Ecophysiological examination of the Lake Erie Microcystis bloom in 2014: linkages between biology and the water supply shutdown of Toledo, OH. *Environ. Sci. Technol.* **51** (12), 6745–6755 (2017).
45. McKindles, K. M. et al. Dissolved microcystin release coincident with lysis of a bloom dominated by Microcystis spp. in western Lake Erie attributed to a novel cyanophage. *Appl. Environ. Microbiol.* **86**, e01397–e01320. 0.1128/AEM.01397-20 (2020).
46. Maslov, S. & Sneppen, K. Population cycles and species diversity in dynamic kill-the-winner model of microbial ecosystems. *Sci. Rep.* **7**, 1–8. https://doi.org/10.1038/srep39642 (2017).
47. Tokodi, N. et al. Protected freshwater ecosystem with incessant cyanobacterial blooming awaiting a resolution. *Water* **12**, 129 (2019).
48. Jia, N. et al. Interspecific competition reveals *Raphidiopsis Raciborskii* as a more successful invader than. *Microcystis aeruginosa Harmful Algae*. **97**, 101858 (2020).
49. Laloum, E. et al. Isolation and characterization of a novel Lambda-like phage infecting the bloom-forming cyanobacteria *Cylindrospermopsis Raciborskii*. *Environ. Microbiol.* **24**, 2435–2448 (2022).
50. Yoshida, T. et al. Isolation and characterization of a cyanophage infecting the toxic cyanobacterium *Microcystis aeruginosa*. *Appl. Environ. Microbiol.* **72**, 1239–1247 (2006).
51. Andersson, A. F. & Banfield, J. F. Virus population dynamics and acquired virus resistance in natural microbial communities. *Science* **320**, 1047–1050 (2008).
52. Martiny, J. B., Riemann, L., Marston, M. F. & Middelboe, M. Antagonistic coevolution of marine planktonic viruses and their hosts. *Annu. Rev. Mar. Sci.* **6**, 393–414 (2014).
53. Middelboe, M. Bacterial growth rate and marine virus–host dynamics. *Microb. Ecol.* **40**, 114–124 (2000).
54. Wang, I. N., Dykhuizen, D. E. & Slobodkin, L. B. The evolution of phage lysis timing. *Evol. Ecol.* **10**, 545–558 (1996).
55. Wang, I. N. Lysis timing and bacteriophage fitness. *Genetics* **172**, 17–26 (2006).

56. Weitz, J. S. et al. Phage-bacteria infection networks. *Trends Microbiol.* **21**, 82–91 (2013).
57. Våge, S., Storesund, J. E. & Thingstad, T. F. Adding a cost of resistance description extends the ability of virus-host model to explain observed patterns in structure and function of pelagic microbial communities. *Environ. Microbiol.* **15**, 1842–1852 (2013).
58. Zhao, D. et al. Network analysis reveals seasonal variation of co-occurrence correlations between Cyanobacteria and other bacterioplankton. *STOTEN* **573**, 817–825 (2016).
59. Coloma, S., Gaedke, U., Sivonen, K. & Hiltunen, T. Frequency of virus-resistant hosts determines experimental community dynamics. *Ecology* **100**, e02554 (2019).
60. Zhang, J. & Shakhnovich, E. I. Slowly replicating lytic viruses: pseudolysogenic persistence and within-host competition. *Phys. Rev. Lett.* **102** (17), 178103. https://doi.org/10.1103/PhysRevLett.102.178103 (2009).
61. Correa, A. M. S. et al. Revisiting the rules of life for viruses of microorganisms. *Nat. Rev. Microbiol.* **19**, 501–513 (2021).
62. Suttle, C. A. & Chan, A. M. Marine cyanophages infecting oceanic and coastal strains of *Synechococcus*: abundance, morphology, cross-infectivity and growth characteristics. *Mar. Ecol. Prog Ser.* **92**, 99–109. https://doi.org/10.3354/meps092099 (1993).
63. Makarova, K. S., Wolf, Y. I., Snir, S. & Koonin, E. V. Defense islands in bacterial and archaeal genomes and prediction of novel defense systems. *J. Bacteriol.* **193**, 6039–6056 (2011).
64. Zborowsky, S. & Lindell, D. Resistance in marine cyanobacteria differs against specialist and generalist cyanophages. *Proc. Natl. Acad. Sci.* **116**, 16899–16908 (2019).
65. Kimura, S. et al. Diurnal infection patterns and impact of *Microcystis* cyanophages in a Japanese pond. *Appl. Environ. Microbiol.* **78**, 5805–5811 (2012).
66. Flores, C. O. et al. Statistical structure of host-phage interactions. *Proc. Natl. Acad. Sci. U.S.A.* 108, 1–10 (2011).
67. Finke, J. F. & Suttle, C. A. The environment and cyanophage diversity: insights from environmental sequencing of DNA polymerase. *Front. Microbiol.* **10**, 167 (2019).
68. Sabart, M., Quiblier, C., Briand, E., Escoffier, N. & Pascal, B. Spatiotemporal changes in the genetic diversity of a bloom-forming *Microcystis aeruginosa* (cyanobacteria) population. *ISME J.* **3**, 419–429 (2009).
69. Bertos-fortis, M. et al. Unscrambling cyanobacteria community dynamics related to environmental factors. *Front. Microbiol.* **7**, 625 (2016).
70. Tokodi, N. et al. Mechanisms responsible for the ubiquity of cyanobacterium *Raphidiopsis raciborskii* – is photosynthetic apparatus a key player? *Algal Res.* **85**, 103870 (2025).
71. Šulčius, S. et al. Insights into cyanophage-mediated dynamics of nodularin and other non-ribosomal peptides in *Nodularia spumigena*. *Harmful Algae*. **78**, 69–74 (2018).
72. Morimoto, D., Kimura, S., Sako, Y. & Yoshida, T. Transcriptome analysis of a bloom-forming cyanobacterium *Microcystis aeruginosa* during Ma-LMM01 phage infection. *Front. Microbiol.* **9**, 2 (2018).
73. Wei, N., Hu, C., Dittmann, E., Song, L. & Gan, N. The biological functions of microcystins. *Water Res.* **262**, 122119 (2024).
74. Hernando, M. et al. Physiological responses and toxin production of Microcystis aeruginosa in short-term exposure to solar UV radiation. *Photoch Photobio Sci.* **17**, 69–80 (2018).
75. Malanga, G., Giannuzzi, L. & Hernando, M. The possible role of microcystin (D-Leu1 MC-LR) as an antioxidant on Microcystis aeruginosa (Cyanophyceae). In vitro and in vivo evidence. *Comp. Biochem. Phys. C.* **225**, 108575 (2019).
76. Stark, G. F. et al. Microcystin aids in cold temperature acclimation: differences between a toxic Microcystis wildtype and non-toxic mutant. *Harmful Algae*. **129**, 102531 (2023).
77. Stucken, K., John, U., Cembella, A., Soto-Liebe, K. & Vásquez, M. Impact of nitrogen sources on gene expression and toxin production in the diazotroph *Cylindrospermopsis raciborskii* CS-505 and non-diazotroph *Raphidiopsis brookii* D9. *Toxins* **6**, 1896–1915 (2014).
78. Suominen, S., Brauer, V. S., Rantala-Ylinen, A., Sivonen, K. & Hiltunen, T. Competition between a toxic and a non-toxic Microcystis strain under constant and pulsed nitrogen and phosphorus supply. *Aquat. Ecol.* **51**, 117–130 (2017).
79. Avrani, S., Schwartz, D. A. & Lindell, D. Virus-host swinging party in the oceans: incorporating biological complexity into paradigms of antagonistic coexistence. *Mob. Genetic Elem.* **2** (2), 88–95 (2012).
80. Kolan, D. et al. Tradeoffs between phage resistance and nitrogen fixation drive the evolution of genes essential for cyanobacterial heterocyst functionality. *ISME J.* **18**, wrad008 (2024).
81. Provasoli, L. & Pinter, I. J. Artificial media for fresh-water algae: problems and suggestions. In *The Ecology of Algae* (Eds. Tryon, C.A. & Hartmann, R.T.) 84–96. University of Pittsburgh (1959).
82. Guillard, R. R. L. & Lorenzen, C. J. Yellow-green algae with chlorophyllide C12. *J. Phycol.* **8**, 10–14 (1972).
83. Rippka, R., Deruelles, J., Waterbury, J. B., Herdman, M. & Stanier, R. Y. Generic assignments, strain histories and properties of pure cultures of cyanobacteria. *J. Gen. Microbiol.* **111**, 1–61 (1979).
84. Govindjee. Chlorophyll a Fluorescence: A Bit of Basics and History. In: Papageorgiou, G.C., Govindjee (eds) Chlorophyll a Fluorescence. Advances in Photosynthesis and Respiration, vol 19. Springer, Dordrecht. https://doi.org/10.1007/978-1-4020-3218-9_1 (2004).
85. Meriluoto, J. et al. TOXIC: cyanobacterial monitoring and cyanotoxin analysis (2005).
86. Dziga, D., Kokocinski, M., Maksylewicz, A., Czaja-Prokop, U. & Barylski, J. Cylindrospermopsin biodegradation abilities of Aeromonas sp. isolated from Rusałka Lake. *Toxins* **8** (3), 55 (2016).
87. Dziga, D., Wladyka, B., Zielińska, G., Meriluoto, J. & Wasylewski, M. Heterologous expression and characterisation of microcystinase. *Toxicon* **59** (5), 578–586 (2012).
88. Spoof, L. et al. First observation of cylindrospermopsin in Anabaena lapponica isolated from the boreal environment (Finland). *Environ. Toxicology: Int. J.* **21** (6), 552–560 (2006).

Acknowledgements

Authors acknowledge the invaluable contributions of the students Robert Maziarz and Baris Tanriverdi who worked on this research project whose dedication, hard work, and enthusiasm have greatly enriched the presented findings. Furthermore, authors would like to thank Anusuya Willis for providing the Raphidiopsis raciborskii CS-505 and CS-506 strains supplied from the Australian National Algae Culture Collection (Hobart, Australia).

Author contributions

D.D. and Š.S. designed the study; N.T., A.Ł., A.A., S.M. performed analyses; S.A. provided Raphidiopsis raciborskii KLL07 and Cr-LKS4; T.Y. provided Microcystis aeruginosa NIES-298 and Ma-LMM01; B.K., Š.S. contributed to analyses; D.D., N.T. wrote the original draft; D.D., N.T. S.A., S.Š., T.Y. contributed substantially to revisions. All authors read and approved the final manuscript.

Funding

This work was funded by the Research Council of Lithuania (LMTLT), agreement No (S-LL-21-10) and the National Science Centre, Poland (project No 2020/38/L/NZ9/00135; 2021/41/N/NZ9/02957). Nada Tokodi was

supported by postdoctoral funding from Narodowa Agencja Wymiany Akademickiej (NAWA) with ULAM grant number PPN/ULM/2019/1/00219. Sarit Avrani was supported by the Israel Science Foundation (grant number 1386/20). The open-access publication has been supported by the Faculty of Biochemistry, Biophysics and Biotechnology under the Strategic Programme Excellence Initiative at Jagiellonian University in Krakow, Poland.

Declarations

Competing interests

The authors declare no competing interests.

Additional information

Supplementary Information The online version contains supplementary material available at https://doi.org/10.1038/s41598-025-87626-z.

Correspondence and requests for materials should be addressed to D.D.

Reprints and permissions information is available at www.nature.com/reprints.

Publisher's note Springer Nature remains neutral with regard to jurisdictional claims in published maps and institutional affiliations.

Open Access This article is licensed under a Creative Commons Attribution-NonCommercial-NoDerivatives 4.0 International License, which permits any non-commercial use, sharing, distribution and reproduction in any medium or format, as long as you give appropriate credit to the original author(s) and the source, provide a link to the Creative Commons licence, and indicate if you modified the licensed material. You do not have permission under this licence to share adapted material derived from this article or parts of it. The images or other third party material in this article are included in the article's Creative Commons licence, unless indicated otherwise in a credit line to the material. If material is not included in the article's Creative Commons licence and your intended use is not permitted by statutory regulation or exceeds the permitted use, you will need to obtain permission directly from the copyright holder. To view a copy of this licence, visit http://creativecommons.org/licenses/by-nc-nd/4.0/.

© The Author(s) 2025